Generalized moment expansion for observables of stochastic processes in dimensions $d>1$: Application to Mössbauer spectra of proteins

Cite as: J. Chem. Phys. **84**, 4015 (1986); https://doi.org/10.1063/1.450061
Submitted: 26 August 1985 . Accepted: 24 September 1985 . Published Online: 31 August 1998

Walter Nadler, and Klaus Schulten

Generalized moment expansion for observables of stochastic processes in dimensions $d > 1$: Application to Mössbauer spectra of proteins

Walter Nadler and Klaus Schulten
Physik Department der Technischen Universität München, 8046 Garching, Federal Republic of Germany

(Received 26 August 1985; accepted 24 September 1985)

The generalized moment expansion provides an effective algorithm for the approximation of the time dependence of observables that monitor stochastic processes. Up to now this method had been applied mainly to one-variable birth–death processes or to one-dimensional Fokker–Planck systems since in these cases analytical and numerical methods for the evaluation of the generalized moments were available. Here we demonstrate that numerical sparse matrix methods can be used to extend the range of application of the generalized moment expansion to higher dimensions. For this purpose we introduce a simple but general discretization scheme for Fokker–Planck operators of Smoluchowski type which is, for these special operators, superior to common numerical discretization schemes for differential operators. As an application we determine the Mössbauer absorption spectrum of a Brownian particle in certain two- and three-dimensional potentials. This serves as a model for the motion of the heme group in myoglobin.

I. INTRODUCTION

Dynamical processes in condensed phase systems can often be modeled to a satisfactory degree as stochastic processes and are, therefore, described mathematically by means of Fokker–Planck equations (or the corresponding Langevin equations) or by their discrete analog, master equations.[1–4] Examples for the successful application of such a description range from transport phenomena in liquids and solids,[4–6] even at phase transitions,[7] to the behavior of chemical reaction systems[1] and of macroscopic quantum systems, e.g., lasers.[2,3] Our own interest in this field arose from the fact that also in macromolecular systems of biological origin it is possible to regard transport processes as stochastic. Such processes range from the active and passive transport of biomolecules in cells and cell compartments[8,9] to the motion of atoms and side groups inside protein molecules[10] and during the process of protein folding.[11]

Transport processes can be monitored through the observation of certain observables. Most often the long-time or, respectively, the low-frequency behavior of these observables is of interest. However, mathematical models for stochastic processes admit analytical solutions only for very simple cases and the numerical long-time integration of the differential equations governing stochastic transport is often time consuming and susceptible to numerical errors. For this purpose a simple and effective approximation procedure has been developed which can reproduce the short- as well as the long-time behavior of observables correctly.[12] This method is based on the *generalized moment expansion* (GME) of observables and is an extension of the first passage time approximation,[4,13–15] usually used for the description of diffusion-controlled reactive processes. The approximation requires the evaluation of the generalized moments which determine the short- and long-time behavior of the observables. The GME has already been used successfully for the approximate description of observables in rather different situations of stochastic transport: the fluorescence yield in continuous fluorescence microphotolysis[16] monitoring lateral diffusion in membranes, the Mössbauer absorption spectrum of Brownian particles[17] and of proteins,[18] and to the relaxation of equilibrium correlation functions in nonreactive Brownian processes[19] and in the stationary state of autocatalytic chemical reaction systems.[20]

However, up to now the application of the GME has been limited to transport problems which can be described by *one-dimensional* stochastic processes, i.e., one-variable birth–death processes and one-dimensional Fokker–Planck systems. In these situations the evaluation of the generalized moments, which involves the solution of inhomogeneous linear partial differential equations, is rather straightforward since analytical results[19] or numerical methods[16,17,19] are available. These numerical methods involve a discretization of the Fokker–Planck operator and, hence, lead to a system of inhomogeneous linear equations to be solved numerically for the determination of the generalized moments. In more general situations common numerical methods for the solution of systems of linear equations fail because of the high dimension of the matrices that arise from the discretization. However, these matrices contain mostly zeroes, i.e., are *sparse*. In recent years there have been developed both direct and iterative numerical algorithms to solve systems of linear equations which involve large *sparse matrices* (see, e.g., Refs. 21 and 22). This development will be exploited in the following paper. We will present an algorithm for the numerical evaluation of the generalized moments that is applicable also in higher-dimensional situations and employs sparse matrix methods. The algorithm will be tested on the Mössbauer line shape of Brownian particles moving in two- and three-dimensional potentials which result from interactions inside a protein.

The paper is organized as follows: In Sec. II we define the stochastic processes and observables considered and give a short review of the GME and the approximation based on it. Nonreactive and reactive processes, up to now considered only separately in publications on GME, will be treated together. In Sec. III we apply the GME to Fokker–Planck systems in higher dimensions. For this purpose we suggest a discretization scheme of Fokker–Planck operators of Smo-

 0021-9606/86/074015-11$02.10

luchowski type and discuss the numerical evaluation of the generalized moments. Finally, in Sec. IV, we will apply the methods of the preceding sections to evaluate the Mössbauer absorption spectrum of a Brownian particle which models the motion of the heme group in the protein myoglobin.

II. STOCHASTIC PROCESSES AND GENERALIZED MOMENT EXPANSION OF OBSERVABLES

We consider stochastic processes in a d-dimensional space V which may be finite or infinite. It will be useful to draw a distinction between nonreactive and reactive processes.

In the nonreactive case, the time evolution of the continuous probability distribution $p(\mathbf{x},t\,|\mathbf{x}_0)$ is determined by the Fokker–Planck equation (FPE)

$$\frac{\partial}{\partial t}p(\mathbf{x},t\,|\mathbf{x}_0)=L(\mathbf{x})\,p(\mathbf{x},t\,|\mathbf{x}_0) \tag{2.1a}$$

with initial condition

$$p(\mathbf{x},t=0|\mathbf{x}_0)=\delta(\mathbf{x}-\mathbf{x}_0)\,, \tag{2.1b}$$

and a Fokker–Planck operator (FPO) of Smoluchowski type

$$L(\mathbf{x})=\nabla\cdot D(\mathbf{x})\{\nabla+\beta\,[\nabla U(\mathbf{x})]\}\,. \tag{2.1c}$$

These equations describe a diffusion process in a potential $U(\mathbf{x})$ with a diffusion coefficient $D(\mathbf{x})$ which may be in general position-dependent but must not vanish anywhere. $\beta=1/k_BT$ is the inverse temperature. An FPO of type (2.1c) is encountered in most situations where detailed balance (see, e.g., Refs. 2 and 3) holds. In a nonreactive process the total probability of the system is conserved. In case of an infinite diffusion space the probability current

$$\mathbf{j}(\mathbf{x})=D(\mathbf{x})\{\nabla+\beta[\nabla U(\mathbf{x})]\}p(\mathbf{x},t\,|\mathbf{x}_0) \tag{2.2}$$

must vanish then at infinity:

$$\lim_{\mathbf{x}\to\infty}\mathbf{j}(\mathbf{x})=\mathbf{0}\,. \tag{2.3a}$$

In case the diffusion space V is finite, the component of $\mathbf{j}(\mathbf{x})$ perpendicular to the surface ∂V of V has to vanish, i.e.,

$$\mathbf{n}(\mathbf{x})\cdot\mathbf{j}(\mathbf{x})|_{\mathbf{x}\in\partial V,\,\mathbf{n}\perp\partial V}=0\,. \tag{2.3b}$$

Boundary conditions (2.3) guarantee that the thermal distribution

$$p_0(\mathbf{x})=N^{-1}\exp[-\beta U(\mathbf{x})]\,, \tag{2.4}$$

with N a normalization constant, is the unique stationary solution of Eq. (2.1). Averages with respect to $p_0(\mathbf{x})$ will be denoted by $\langle\ \rangle$. For Eq. (2.1) to be ergodic we require that the part of V where $p_0(\mathbf{x})$ does not vanish is connnected, i.e., there are no potential walls of infinite height separating different parts of V. With the help of Eq. (2.4) we can bring the FPO (2.1c) into the convenient form

$$L(\mathbf{x})=\nabla\cdot D(\mathbf{x})\,p_0(\mathbf{x})\nabla p_0(\mathbf{x})^{-1}\,. \tag{2.5}$$

In reactive stochastic processes, the total probability for the presence of a particle undergoing a diffusive motion described by Eq. (2.1) decreases with time due to reactions either at the boundary and/or inside V. We will limit ourselves to reactions of first order. Such reactions *at the boundary* are described by supplying Eq. (2.1) with radiation boundary conditions[2,3,13]:

$$\mathbf{n}(\mathbf{x})\cdot\mathbf{j}(\mathbf{x})|_{\mathbf{x}\in\partial V,\,\mathbf{n}\perp\partial V}=k(\mathbf{x})\,p(\mathbf{x},t\,|\mathbf{x}_0)|_{\mathbf{x}\in\partial V}\,, \tag{2.6}$$

where $k(\mathbf{x})$ is a, possibly position-dependent reaction rate coefficient defined at the boundary and $\mathbf{n}(\mathbf{x})$ a unit vector pointing out of V. For $k\to0$ one retains the nonreactive case, whereas $k\to\infty$ implies that a reaction occurs with certainty if a diffusing particle reaches the boundary. Unimolecular reactions *inside* V are described by adding the reaction rate $k(\mathbf{x})$, now defined inside V, as a reactive (optical) potential $-k(\mathbf{x})$ to the FPO

$$L(\mathbf{x})\to L(\mathbf{x})-k(\mathbf{x})\,. \tag{2.7}$$

For notational convenience we will denote reactive processes solely by the FPO (2.7), even if the reaction rate $k(\mathbf{x})$ is nonvanishing only at the boundary ∂V. In reactive processes the probability distribution vanishes for $t\to\infty$ and, therefore, $p_0(\mathbf{x})$ is not the stationary distribution. However, since the diffusive motion is still determined by the potential $U(\mathbf{x})$, we can view $p_0(\mathbf{x})$ as a quasistationary distribution which is valid for very long times in the limit $k\to0$.

Observables of the stochastic processes defined above assume, in general, the form

$$M(t)=\int_V d^dx\int_V d^dx_0\,f(\mathbf{x})\,p(\mathbf{x},t\,|\mathbf{x}_0)\,g_0(\mathbf{x}_0)\,, \tag{2.8}$$

where $g_0(\mathbf{x}_0)$ is determined by the preparation of the stochastic system and $f(\mathbf{x})$ denotes how the system is monitored. In most experimental situations, even in case of reactive processes, the initial distribution of the system is given by the thermal or quasistationary distribution $p_0(\mathbf{x}_0)$. We therefore write $g_0(\mathbf{x}_0)$ in the form

$$g_0(\mathbf{x}_0)=g(\mathbf{x}_0)\,p_0(\mathbf{x}_0)\,. \tag{2.9}$$

$M(t)$ can then be viewed as an equilibrium correlation function

$$M(t)=\langle\langle f[\mathbf{x}(t)]\,g[\mathbf{x}(0)]\rangle\rangle\,, \tag{2.10}$$

where $\langle\langle\ \rangle\rangle$ denotes the average over the process (2.1) *and* over thermal initial conditions.

With the use of the adjoint FPO L^+,[2,3,13] which in analogy to Eq. (2.5) can be written as

$$L^+(\mathbf{x})=p_0(\mathbf{x})^{-1}\,\nabla\cdot D(\mathbf{x})\,p_0(\mathbf{x})\nabla\,, \tag{2.11}$$

the observable $M(t)$ can be expressed in a formal way as an expectation value with respect to $p_0(\langle\cdots\rangle=\int_V d^dx\,p_0(\mathbf{x})\cdots)$,

$$M(t)=\langle\,g(\mathbf{x})\exp[L^+(\mathbf{x})t\,]\,f(\mathbf{x})\rangle\,. \tag{2.12}$$

In case of reactive processes one gets

$$M(t)=\langle g(\mathbf{x})\exp\{\,[L^+(\mathbf{x})-k(\mathbf{x})]t\,\}\,f(\mathbf{x})\rangle\,. \tag{2.13}$$

The adjoint operator L^+ is always confined to the function space given by the adjoint boundary conditions,[2,3,13] i.e., for nonreactive processes

$$\mathbf{n}(\mathbf{x})\cdot D(\mathbf{x})\nabla f(\mathbf{x})|_{\mathbf{x}\in\partial V,\,\mathbf{n}\perp\partial V}=0 \tag{2.14a}$$

or

$$\lim_{\mathbf{x}\to\infty}D(\mathbf{x})\nabla f(\mathbf{x})=\mathbf{0}\,, \tag{2.14b}$$

respectively, and for reactive processes

$$\mathbf{n}(\mathbf{x})\cdot D(\mathbf{x})\nabla f(\mathbf{x})|_{\mathbf{x}\in\partial V,\,\mathbf{n}\perp\partial V}=k(\mathbf{x})\,f(\mathbf{x})|_{\mathbf{x}\in\partial V}\,. \tag{2.15}$$

If transport processes are monitored with a finite time

resolution γ^{-1}, as is the case with observations of particles or excitations with a finite lifetime, e.g., in Mössbauer spectroscopy (see Sec. IV), the observable assumes the form

$$M(t) = e^{-\gamma t}\langle\langle f[\mathbf{x}(t)]\, g[\mathbf{x}(0)]\rangle\rangle$$
$$= \langle g(\mathbf{x})\exp\{[L^{+}(\mathbf{x}) - \gamma]t\}\, f(\mathbf{x})\rangle\,. \quad (2.16)$$

This demonstrates that observations with a finite time resolution γ^{-1} are equivalent to reactive processes with a constant reactive potential γ.

In case of nonreactive processes the observable $M(t)$ relaxes from the initial value

$$M(0) = \langle f(\mathbf{x})\, g(\mathbf{x})\rangle \quad (2.17a)$$

to the value

$$M(\infty) = \langle f(\mathbf{x})\rangle\langle g(\mathbf{x})\rangle \quad (2.17b)$$

in the limit $t\to\infty$. In general $M(\infty)$ does not vanish. For an analysis of the time behavior of $M(t)$ it is sufficient to consider only the *relaxational contribution* to $M(t)$, i.e., the difference

$$\Delta M(t) = M(t) - M(\infty)\,. \quad (2.18)$$

Using the projection operator

$$J_0^{+}(\mathbf{x})\, f(\mathbf{x}) = \int_V d^d x'\, f(\mathbf{x}')\, p_0(\mathbf{x}') = \langle f(\mathbf{x})\rangle\,, \quad (2.19)$$

which projects onto the *kernel* of the adjoint operator L^{+}, we can restrict L^{+} to the part of its function space that lies outside its kernel

$$\{L^{+}(\mathbf{x})\}_{\perp}^{+} = [1 - J_0^{+}(\mathbf{x})]L^{+}(\mathbf{x})[1 - J_0^{+}(\mathbf{x})]\,.$$

Employing this method of restricting the function space (compare Ref. 19), the formal expression for $\Delta M(t)$, in analogy to Eq. (2.12), is

$$\Delta M(t) = \langle g(\mathbf{x})\{\exp[L^{+}(\mathbf{x})t]\}_{\perp}^{+} f(\mathbf{x})\rangle\,. \quad (2.21)$$

Since $M(\infty) = 0$ for reactive processes, the relaxational contribution $\Delta M(t)$ is identical with $M(t)$ for these processes. For notational convenience we solely use $\Delta M(t)$ in the remaining part of this paper to denote both Eqs. (2.13) and (2.21).

Starting point of the GME is the Laplace transform of the observable $\Delta M(t)$:

$$\Delta\tilde{M}(\omega) = \int_0^{\infty} dt\, e^{-\omega t}\Delta M(t)\,, \quad (2.22)$$

for which, in case of nonreactive processes, we obtain the formal expression

$$\Delta\tilde{M}(\omega) = \langle g(\mathbf{x})\{[\omega - L^{+}(\mathbf{x})]^{-1}\}_{\perp}^{+} f(\mathbf{x})\rangle\,. \quad (2.23a)$$

The corresponding expression in case of reactive processes is

$$\Delta\tilde{M}(\omega) = \langle g(\mathbf{x})[\omega + k(\mathbf{x}) - L^{+}(\mathbf{x})]^{-1} f(\mathbf{x})\rangle\,. \quad (2.23b)$$

$\Delta M(\omega)$ can be expanded for low and high frequencies:

$$\Delta\tilde{M}(\omega) \underset{\omega\to\infty}{\sim} \omega^{-1}\sum_{n=0}^{\infty}\mu_n(-\omega)^{-n}\,, \quad (2.24a)$$

$$\Delta\tilde{M}(\omega) \underset{\omega\to 0}{\sim} \sum_{n=0}^{\infty}\mu_{-n-1}(-\omega)^{n}\,, \quad (2.24b)$$

where the expansion coefficients, the *generalized moments*, are given by

$$\mu_n = (-1)^n\langle g(\mathbf{x})\{[L^{+}(\mathbf{x})]^n\}_{\perp}^{+} f(\mathbf{x})\rangle\,, \quad (2.25a)$$

in case of nonreactive processes, and by

$$\mu_n = (-1)^n\langle g(\mathbf{x})[L^{+}(\mathbf{x}) - k(\mathbf{x})]^n f(\mathbf{x})\rangle\,, \quad (2.25b)$$

in case of reactive processes. It is important to note that the generalized moments μ_n are well defined for $n\geqslant 0$ as well as for $n<0$. A general numerical method for the determination of the generalized moments will be presented in the next section.

Once the μ_n are known, they can be used for the construction of an approximation $\Delta\tilde{m}(\omega)$ to $\Delta\tilde{M}(\omega)$. A very promising functional form for $\Delta\tilde{m}(\omega)$ is a series of N Lorentzians

$$\Delta\tilde{m}(\omega) = \sum_{n=0}^{N-1} f_n[\omega + \Gamma_n]^{-1}\,, \quad (2.26)$$

which represents an $[N-1, N]$ Padé approximant. $\Delta\tilde{m}(\omega)$ should describe the low- and high-frequency behavior [Eq. (2.24)] of $\Delta\tilde{M}(\omega)$ correctly. We therefore require that $\Delta\tilde{m}(\omega)$ reproduces the first N_h high and the first N_l low-frequency moments μ_n. With this requirement Eq. (2.26) represents a two-sided Padé approximation[23] of $\Delta\tilde{M}(\omega)$ around $\omega = 0$ and $\omega^{-1} = 0$ and we call it a (N_h, N_l)-*generalized moment approximation*. The sum of N_h and N_l must be even, i.e., $N_h + N_l = 2N$. The parameters f_n and Γ_n of Eq. (2.26) are determined from the generalized moments through the relations

$$\sum_{n=0}^{N-1} f_n\,\Gamma_n^m = \mu_m\,, \quad m = -N_l, -N_l+1, \ldots, N_h - 1\,. \quad (2.27)$$

An algorithm for the solution of these nonlinear equations is given in Refs. 12 and 16.

We may stress that in practical applications mainly the low-frequency moments are responsible for the characteristic features of the temporal behavior of observables.[16–20] Therefore, the generalized moments for $n<0$ must be included primarily in the approximation and their evaluation is of special importance.

III. NUMERICAL DETERMINATION OF GENERALIZED MOMENTS

As a first step for the evaluation of the generalized moments defined in Eq. (2.25) it is useful to introduce auxiliary functions $\mu_n(\mathbf{x})$ through

$$\mu_n(\mathbf{x}) = (-1)^n\{[L^{+}(\mathbf{x})]^n\}_{\perp}^{+} f(\mathbf{x})\,, \quad n\neq 0\,, \quad (3.1a)$$
$$\mu_0(\mathbf{x}) = f(\mathbf{x}) - \langle f(\mathbf{x})\rangle,$$

in the nonreactive case and

$$\mu_n(\mathbf{x}) = (-1)^n[L^{+}(\mathbf{x}) - k(\mathbf{x})]^n f(\mathbf{x})\,, \quad n\neq 0\,, \quad (3.1b)$$
$$\mu_0(\mathbf{x}) = f(\mathbf{x})\,,$$

in the reactive case. It is clear from Eq. (2.25) that the generalized moments can be calculated easily from these auxiliary functions by the use of the relation

$$\mu_n = \langle g(\mathbf{x})\,\mu_n(\mathbf{x})\rangle\,. \quad (3.2)$$

For $n>0$, i.e., for the high-frequency moments, one easily sees that the following properties:

$$\mu_n(\mathbf{x}) = -\{L^{+}(\mathbf{x})\}_{\perp}^{+}\,\mu_{n-1}(\mathbf{x})\,, \quad n>0\,, \quad (3.3a)$$

and

$$\mu_n(\mathbf{x}) = -[L^{+}(\mathbf{x}) - k(\mathbf{x})]\,\mu_{n-1}(\mathbf{x})\,, \quad n>0\,, \quad (3.3b)$$

respectively, hold. Hence, the auxiliary functions of the high-frequency moments $\mu_1, \mu_2, \ldots$ can be obtained in an iterative way by successive application of operators $\{L^+(\mathbf{x})\}_\perp^+$ and $[L^+(\mathbf{x}) - k(\mathbf{x})]$, respectively, onto the zeroth auxiliary function $\mu_0(\mathbf{x})$. Though, in principle, this can be done always analytically, actual calculations may become cumbersome. We may note that in Eq. (3.3a) the application of the projection operators $[1 - J_0^+]$ may be dropped since L^+ itself projects onto the function space outside its kernel.

For $n < 0$, i.e., for the low-frequency moments, by multiplication of Eq. (3.1) with the respective operator from the *lhs* one obtains the partial differential equations:

$$\{L^+(x)\}_\perp^+ \mu_{-n}(\mathbf{x}) = -\mu_{-(n-1)}(\mathbf{x}), \quad n>0, \quad (3.4a)$$

and

$$[L^+(\mathbf{x}) - k(\mathbf{x})]\,\mu_{-n}(\mathbf{x}) = -\mu_{-(n-1)}(\mathbf{x}), \quad n>0, \quad (3.4b)$$

respectively. These equations have to be solved using the respective boundary conditions (2.14) and (2.15) for the adjoint operator L^+. We may note that the solution of Eq. (3.4a) for the nonreactive processes is equivalent to the solution of the corresponding differential equation with the unrestricted operator L^+,

$$L^+(\mathbf{x})\mu_{-n}(\mathbf{x}) = -\mu_{-(n-1)}(\mathbf{x}), \quad n>0, \quad (3.4a')$$

where the solution $\mu_{-n}(\mathbf{x})$ has to fulfill the orthogonality relation

$$J_0^+(\mathbf{x})\mu_{-n}(\mathbf{x}) = 0. \quad (3.5)$$

By successive solution of Eqs. (3.4) the auxiliary functions for the low-frequency moments $\mu_{-1}, \mu_{-2}, \ldots$ can be obtained.

In Ref. 19 we presented a general analytical solution for (3.4a) in case the diffusion space V is one-dimensional. For the reactive case, Eq. (3.4b), even in one dimension, an analytical solution is available only for special situations, e.g., reactions only at the boundary. This latter situation is related to first passage time problems.[13,24] For general reactive one-dimensional systems and for all higher-dimensional systems analytical solutions for $\mu_{-n}(\mathbf{x})$ are not available and a numerical evaluation is necessary. Numerical methods can also bring considerable computational simplifications to the determination of the high-frequency moments. To this end we employ the following discretization procedure for problems (3.3) and (3.4).

We subdivide a d-dimensional rectangle $R^d = L_1 \times L_2 \times \cdots \times L_d$ that encloses V into $N = N_1 \times N_2 \times \cdots N_d$ cells of size δ^d (see Fig. 1). Each cell is identified by a d-tuple $\mathbf{n} = (n_1, n_2, \ldots, n_d)$ and the value of a function corresponding to a cell is represented by its value at a certain position inside the cell. Discretized functions, therefore, can be thought of as vectors $\mathbf{f}$, the N components of which are numbered by $\mathbf{n}$,

$$(\mathbf{f})_\mathbf{n} = f[\mathbf{x}(\mathbf{n})]. \quad (3.6)$$

For the representative discretization points we choose the centers of the cells

$$x_i(n_i) = x_{i,\min} + (2n_i - 1)\delta/2, \quad \begin{matrix} n_i = 1,\ldots,N_i \\ i = 1,\ldots,d \end{matrix} \quad (3.7)$$

With this choice of discretization points a sum over all components of vector $\mathbf{f}$ corresponds to a numerical integration over V according to the midpoint rule.[25] This rule has the same convergence properties as the more common trapezoidal rule. However, in contrast to the trapezoidal rule, there are no special summation weights for the boundary of V which bears some advantages in higher-dimensional calculations.

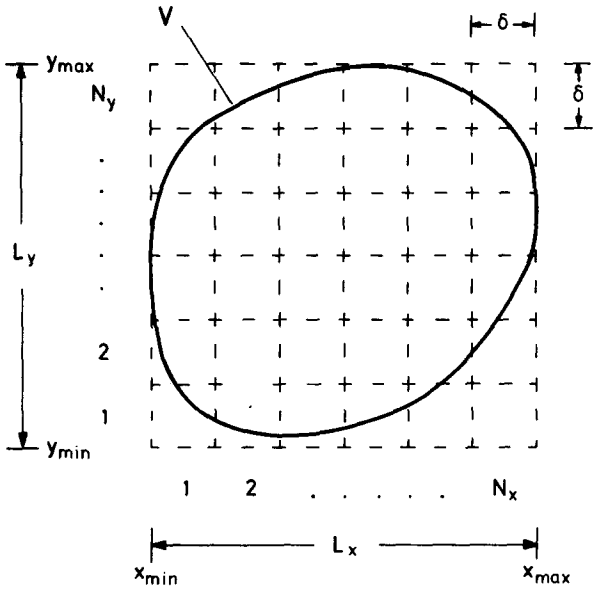

FIG. 1. Partitioning of the diffusion space V into cells in a two-dimensional case.

The common discretization schemes for partial differential operators that are used in numerical mathematics[26–28] have some disadvantages in case of a Fokker–Planck operator L or its adjoint L^+, as is discussed in Appendix A. Therefore, we use an equivalent master equation operator which has the same convergence properties as operators discretized in a common way but, in addition, retains some essential properties of the FPO (compare Appendix A). We first define transition rates between cells

$$W(\mathbf{n}\to\mathbf{m}) = \tau^{-1}[(\mathbf{p}_0)_\mathbf{m}/(\mathbf{p}_0)_\mathbf{n}]^{1/2}, \quad (3.8)$$

where $\mathbf{p}_0$ is the discretized thermal distribution (2.4). Transition rates from or to cells outside of the diffusion space V are required to be zero, corresponding to a vanishing stationary distribution outside V and reflective boundary conditions (2.3), respectively. The time scale τ is given by

$$\tau = \delta^2/D, \quad (3.9)$$

where we have assumed, for simplicity, a constant diffusion coefficient. The more general case employing a position-dependent diffusion coefficient is discussed in Appendix B. Using the transition rates (3.8) we can replace the FPE (2.1) with the master equation

$$\frac{\partial}{\partial t}\mathbf{p} = \mathsf{L}^{(M)}\mathbf{p} \quad (3.10)$$

for a hopping process between the above defined cells. The components of the master equation operator $\mathsf{L}^{(M)}$ are given by

$$L^{(M)}_{\mathbf{n},\mathbf{m}} = \begin{cases} -\sum_{\mathbf{m}' \in N(\mathbf{n})} W(\mathbf{n} \to \mathbf{m}') & \text{for } \mathbf{m} = \mathbf{n}, \\ W(\mathbf{m} \to \mathbf{n}) & \text{for } \mathbf{m} \in N(\mathbf{n}), \\ 0 & \text{otherwise}. \end{cases} \tag{3.11}$$

$N(\mathbf{n})$ is the *neighborhood* of cell $\mathbf{n}$ and denotes the set of cells that share a cell wall with cell $\mathbf{n}$. The above choice of transition rates at the boundary of V guarantees conservation of probability.

Reactive processes are described by a diagonal reaction matrix K with the property

$$K_{\mathbf{n},\mathbf{m}} = \delta_{\mathbf{n},\mathbf{m}} (\mathbf{k})_{\mathbf{n}}, \tag{3.12}$$

where $\delta_{\mathbf{n},\mathbf{m}}$ is the Kronecker symbol and $\mathbf{k}$ is the discretized position-dependent reaction rate. In case reactions occur only at the boundary, this vector has nonvanishing components only for values of $\mathbf{n}$ corresponding to boundary cells, which are those that have cell walls not shared with other cells. The value $(\mathbf{k})_{\mathbf{n}}$ for the discretized reaction rate in boundary cell $\mathbf{n}$ has to be chosen at a representative point of the boundary ∂V inside cell $\mathbf{n}$ so that boundary condition (2.6) is fulfilled. In situations with reactive potential *and* reactive boundary conditions the two respective rates have to be added for boundary cells.

The above defined matrix operator $\mathsf{L}^{(M)}$ has the typical properties of a master equation operator. In particular the following properties hold:

(i) The stationary distribution of Eq. (3.10) is given by $\mathbf{p}_0$, i.e., $\mathbf{p}_0$ is the single eigenvector of $\mathsf{L}^{(M)}$ with eigenvalue zero. In addition, $\mathsf{L}^{(M)}$ obeys the principle of detailed balance with respect to $\mathbf{p}_0$:

$$L^{(M)}_{\mathbf{n},\mathbf{m}} (\mathbf{p}_0)_{\mathbf{m}} = L^{(M)}_{\mathbf{m},\mathbf{n}} (\mathbf{p}_0)_{\mathbf{n}}, \quad \text{for all } \mathbf{n}, \mathbf{m}. \tag{3.13}$$

(ii) The discretized adjoint operator is given by the trans-posed matrix $\mathsf{L}^{(M)T}$,

$$L^{+(M)}_{\mathbf{n},\mathbf{m}} = L^{(M)T}_{\mathbf{n},\mathbf{m}} = L^{(M)}_{\mathbf{m},\mathbf{n}}. \tag{3.14}$$

(iii) The matrix operator $\mathsf{L}^{(M)}$ can be symmetrized by a simple transformation,

$$\mathsf{L}^{(M,s)} = \mathsf{S}^{-1} \mathsf{L}^{(M)} \mathsf{S} = \mathsf{S}\, \mathsf{L}^{+(M)} \mathsf{S}^{-1}, \tag{3.15a}$$

with

$$S_{\mathbf{n},\mathbf{m}} = (\mathbf{p}_0)^{1/2}_{\mathbf{n}} \delta_{\mathbf{n},\mathbf{m}}. \tag{3.15b}$$

This transformation leaves the diagonal terms $L_{\mathbf{n},\mathbf{n}}$ invariant; the other components assume the simple form

$$L^{(M,s)}_{\mathbf{n},\mathbf{m}} = \begin{cases} \tau^{-1} & \text{for } \mathbf{m} \in N(\mathbf{n}), \\ 0 & \text{otherwise}. \end{cases} \tag{3.16}$$

We may note that for actual calculations an infinite diffusion space V has to be limited to a finite one by introducing a boundary. This boundary has to be chosen in such a way, that the essential part of the stationary distribution is included and, therefore, depends on the potential $U(\mathbf{x})$; see Sec. IV for a practical example.

Using the above discretization, Eqs. (3.3) and (3.4) for the determination of the auxiliary functions $\mu_n(\mathbf{x})$ are changed into systems of linear equations.

The discretized auxiliary functions μ_n of the high-frequency moments are determined iteratively from

$$\mu_n = -\mathsf{L}^{+(M)} \mu_{n-1}, \quad n > 0, \tag{3.17a}$$
$$\mu_0 = \mathbf{f} - \langle f \rangle \mathbf{1}$$

in the nonreactive and

$$\mu_n = -[\mathsf{L}^{+(M)} - \mathsf{K}]\, \mu_{n-1} \quad n > 0, \tag{3.17b}$$
$$\mu_0 = \mathbf{f}$$

in the reactive case. Here $\mathbf{1}$ represents the vector with all components unity. The expectation value $\langle f \rangle$ may be calculated from the discretized vector $\mathbf{f}$ by the scalar product $\langle f \rangle = \mathbf{p}_0 \cdot \mathbf{f}$. The evaluation of Eq. (3.17) can be done by simple matrix multiplication and the numerical evaluation poses no special problems.

The differential equations (3.4) for the auxiliary functions of the low-frequency moments are represented now by the linear equations

$$\mathsf{L}^{+(M)} \mu_{-n} = -\mu_{-(n-1)}, \quad n > 0 \tag{3.18a}$$

in the nonreactive case and

$$[\mathsf{L}^{+(M)} - \mathsf{K}]\, \mu_{-n} = -\mu_{-(n-1)}, \quad n > 0 \tag{3.18b}$$

in the reactive case. Equation (3.18b) can be solved in principle in an unequivocal way. This is not the case for Eq. (3.18a) since $\mathsf{L}^{+(M)}$ has the property

$$\mathsf{L}^{+(M)} \mathbf{1} = \mathbf{0}, \tag{3.19}$$

and, therefore, the general solution of Eq. (3.18a) is defined only up to an arbitrary additive vector $c \cdot \mathbf{1}$. The solution we seek must fulfill the discretized orthogonality relation corresponding to Eq. (3.5),

$$\mathsf{J}_0^+ \mu_{-n} = (\mathbf{1}\, \mathbf{p}_0^T)\, \mu_{-n} = \mathbf{0}, \tag{3.20a}$$

where we have represented the projection operator J_0^+ as a dyadic product $(\mathbf{1}\, \mathbf{p}_0^T)$ with $\mathbf{p}_0^T$ the vector transposed to $\mathbf{p}_0$. Condition (3.20a) is equivalent to

$$\mathbf{p}_0 \cdot \mu_{-n} = 0. \tag{3.20b}$$

For the numerical evaluation of Eq. (3.18a) subject to the condition (3.20) the following strategy is useful: One looks for a special solution of Eq. (3.18a) with the property

$$(\mu_{-n})_N = 0, \tag{3.21}$$

where μ_n is assumed to be a vector of dimension N. The solution of Eq. (3.18a) under condition (3.21) is equivalent to the solution of the *reduced* system of linear equations,

$$\mathsf{L}^{+(M),(N-1)} \mu_n^{(N-1)} = -\mu_{-(n-1)}^{(N-1)}. \tag{3.22}$$

In this system the $N \times N$ matrix $\mathsf{L}^{+(M)}$ is replaced by the following $(N-1) \times (N-1)$ matrix,

$$\mathsf{L}^{+(M),(N-1)} = \begin{pmatrix} L^+_{1,1} & \cdots & L^+_{1,N-1} \\ \vdots & & \vdots \\ L^+_{1,N-1} & \cdots & L^+_{N-1,N-1} \end{pmatrix}, \tag{3.23}$$

and the vectors μ_{-n} are replaced by the corresponding vectors without the Nth component. This system of linear equations is solvable in principle in an unequivocal way since it has lost the property (3.19). Using the special solution $\mu_{-n}^{(N-1)}$ the solution of Eq. (3.18a) which obeys condition (3.20) is

$$\underline{\mu}_{-n} = \begin{pmatrix} \underline{\mu}_n^{(N-1)} \\ 0 \end{pmatrix} + c\,\mathbf{1}, \tag{3.24}$$

where the constant c is determined through Eq. (3.20) to

$$c = -\mathbf{p}_0^{(N-1)} \cdot \underline{\mu}_{-n}^{(N-1)}. \tag{3.25}$$

The single remaining problem is the numerical solution of the linear equations (3.18b) and (3.22). In the one-dimensional case the matrix operator $\mathsf{L}^{+(M)}$ has a tridiagonal structure. In this case the well-known Gaussian elimination scheme for the solution of linear equations is very simple and efficient (see, e.g., Ref. 27, p. 198, or Ref. 29, p. 166). We have used this method in earlier applications.[16–19]

In higher-dimensional systems the matrix operator $\mathsf{L}^{+(M)}$ has a more complicated band structure. However, the matrix is sparse since in the d-dimensional case less than $(2d+1)N$ of its N^2 elements are nonvanishing. Therefore it is possible to do calculations for higher-dimensional problems with a considerable number of discretization points using sparse matrix techniques[21,22] for the numerical solution of Eqs. (3.18a) and (3.22).

In the applications of this contribution we used the "Yale Sparse Matrix Package," [30,31] a program package which employs a *direct* method for the numerical solution of the linear equations. It is sufficient for applications to essential two-dimensional systems, as considered here. Since storage requirements of direct methods are relatively large[29] the applications to problems in dimensions greater than two is only possible for simple cases. However there are already available efficient *iterative* algorithms with much fewer storage requirements[32–34] which can be applied in such cases.

An additional reduction in storage requirement and computer time results if one takes advantage of the symmetry transformation (3.15) for the FPO and its adjoint. Equation (3.15) transforms Eq. (3.18) into the symmetric system of linear equations

$$\mathsf{L}^{+(M,s)}\,\underline{\mu}_{-n}^{(s)} = -\underline{\mu}_{-(n-1)}^{(s)} \tag{3.26a}$$

in the nonreactive cases and

$$[\mathsf{L}^{+(M,s)} - \mathsf{K}]\,\underline{\mu}_{-n}^{(s)} = -\underline{\mu}_{-(n-1)}^{(s)} \tag{3.26b}$$

in the reactive case, respectively. Here

$$\underline{\mu}_{-n}^{(s)} = \mathsf{S}\,\underline{\mu}_{-n} \tag{3.27}$$

denotes the symmetrized auxiliary function. In addition, using the symmetrized functions (3.27), relation (3.2) for the last step of the determination of the generalized moments may be written in a rather simple way:

$$\underline{\mu}_{-n} = \mathbf{g}^T\mathsf{S}^2\underline{\mu}_{-n} = \mathbf{g}^{(s)} \cdot \underline{\mu}_{-n}^{(s)}. \tag{3.28}$$

We may note that for the implementation of the above algorithm on a computer it is useful to transform the d-component index $\mathbf{n}$ into a scalar index $\nu^{(d)}$. This can be done in an unequivocal way through the relation

$$\nu^{(d)} = n_1 + \sum_{l=2}^{d} (n_l - 1) \prod_{k=1}^{l-1} N_k, \tag{3.29}$$

where we have assumed $N_1 \geqslant N_2 \geqslant \cdots \geqslant N_d$. The inverse transformation is given by

$$n_1 = 1 + [\nu^{(d)} - 1] \bmod N_1, \tag{3.30a}$$

$$n_l = 1 + \left\{ [\nu^{(d)} - \nu^{(l-1)}] \Big/ \prod_{k=1}^{l-1} N_k \right\} \bmod N_l, \quad l \geqslant 1. \tag{3.30b}$$

However, in case the diffusion space is smaller than the rectangle R^d, the indices of cells outside of V have to be left out and the numbering of $\nu^{(d)}$ has to be changed in an appropriate way.

In closing this section we like to stress that the GME can also be employed if a stochastic system is posed from the outset in terms of a master equation (3.10). This should be evident from the fact that the discretization scheme introduced here has led us to consider a master equation rather than a Fokker–Planck equation. In case the master equation is derived from a FPE (2.1) based on a potential $U(\mathbf{x})$ the detailed balance relation (3.13) holds for the elements of the matrix $\mathsf{L}^{(M)}$. We like to note, however, that the GME described above can also be employed for more general master equations and, correspondingly, also for a FPE with a force term *not* derived from a scalar potential.

IV. APPLICATION: MOTION OF THE HEME GROUP IN MYOGLOBIN

Though proteins are rather densely packed consisting of some 10^2 to 10^4 atoms they are, in particular at physiological temperatures, very flexible and their structure undergoes strong fluctuations.[35–37] There are indications that these structural fluctuations are essential for their enzymatic activity[38,39] and, therefore, there is a growing interest into a deeper understanding of the internal motion of atoms and groups of atoms inside proteins.[10,40] The time scale of the atomic motion is rather short ($\lesssim 1$ ps) and on this time scale the motion of individual atoms displays strong similarities to that in fluids. On longer time scales the individual atoms take part in the concerted motion of larger groups. The motion of such a protein segment can be considered stochastic, with the rest of the protein and the surrounding solvent acting as a heat bath and influencing the motion through noise and frictional forces. This approach bears some similarities to theories considering chemical reactions in solvents.[41] It leads to an effective *one-particle model* which describes the motion of a protein segment along a relevant coordinate $\mathbf{x}$ (e.g., center of mass, rotational angle, etc.) through a Fokker–Planck equation (2.1). The effective potential $U(\mathbf{x})$ and diffusion coefficient D are determined by the surrounding protein.

Frauenfelder *et al.*[36,42] have argued that internal motions of proteins on longer than atomic time scales are mainly due to fluctuations between conformational substates. These conformational substates can be represented by multiminimum potentials and we have discussed such models in one dimension in Refs. 17 and 18. There we demonstrated that the description of the motion can be simplified by using a smoothed potential and an effective diffusion coefficient with an Arrhenius-like temperature dependence. To account correctly for the temperature dependence of observations in case of the motion of the heme group in myoglobin, at least one additional substate of low energy had to be introduced. However, due to the limitations of one-dimensional

models in the description of essential three-dimensional motion, rather unphysical small linear extensions of this substate had to be assumed. In order to demonstrate that this is not the case in higher-dimensional models we supply an extension of our earlier calculations to dimensions $d = 2$ and $d = 3$ using the method presented in this paper.

In our model the diffusive motion of the heme group is determined by a d-dimensional potential, the form of which is sketched qualitatively in Fig. 2. The substates between the dashed lines are represented by an effective diffusion coefficient

$$D_{\text{eff}}(T) = D_0 \exp[-\beta E_0]. \tag{4.1}$$

The smoothed potential is of radial symmetry and consists of an harmonic envelope potential with a superimposed low-energy substate the form of which we choose for simplicity to be Gaussian

$$U_{\text{eff}}(r) = \tfrac{1}{2}(r/r_0)^2 - \Delta E \cdot \exp[-\tfrac{1}{2}(r/s_0)^2]. \tag{4.2}$$

As in Ref. 18 we use $k_B r_0^2 = 3.6\times 10^{-4}$ Å^2/K as the parameter for the harmonic envelope potential. This choice is in accordance with room temperature x-ray data.[36] The representative substate in Eq. (4.2) describes the contributions from energetically low substates whose existence is indicated by low-temperature x-ray data.[36] Altogether, with our model we reduce the description of the stochastic motion of the heme group to four parameters: D_0, E_0 describing the effective diffusion coefficient of the group and s_0, ΔE describing the width and depth of the stable substate.

The motion of the heme group can be monitored through observation of the motion of its central Fe atom by Mössbauer absorption spectroscopy. For ^{57}Fe, Mössbauer spectroscopy can give information on dynamical properties in a time window of about 1–100 ns. The Mössbauer spectrum of a diffusing Fe atom is given by[43,17]

$$I(\omega) = \text{Re}\{\tilde{S}(\mathbf{k}, i\omega)\} \tag{4.3a}$$

with the dynamic structure factor

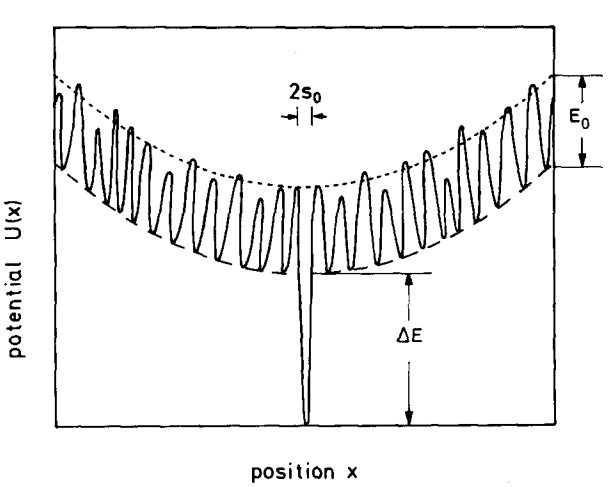

FIG. 2. Sketch of the profile of a microscopic d-dimensional potential that can be approximated by the effective diffusion coefficient (4.1) and the effective potential (4.2).

$$\tilde{S}(\mathbf{k},\omega) = \int_0^\infty dt\, e^{-\omega t} e^{-\Gamma t/2} \langle\langle \exp\{i\,\mathbf{k}\cdot[\mathbf{x}(t) - \mathbf{x}(0)]\}\rangle\rangle. \tag{4.3b}$$

We have chosen $\int_{-\infty}^{\infty} d\omega I(\omega) = \pi$ as normalization of the spectrum. $\mathbf{k}$ is the momentum of the absorbed γ quantum with $|\mathbf{k}| = 7.3$ Å^{-1}. $\Gamma = 7.0\times 10^6$ s^{-1} is the lifetime of the excitation of the ^{57}Fe nucleus. From Eq. (4.3b) it is clear that the structure factor is an observable of type (2.16). Therefore, an approximation of the spectrum can be made using the GME with the monitoring functions $f(\mathbf{x}) = g^*(\mathbf{x}) = \exp(i\,\mathbf{k}\cdot\mathbf{x})$ and a constant reactive term $\Gamma/2$. It has been demonstrated in Refs. 17 and 18 that a 3-Lorentzian description of the spectrum using a (1,5)-generalized moment approximation (see Sec. II), i.e., employing mainly low-frequency moments, is sufficient for a comparison with the observations. From Eq. (2.26) it can be seen that such an approximate absorption spectrum has the form

$$I(\omega) = 2\sum_{n=0}^{2} \Gamma_n\, f_n (\Gamma_n^2 + \omega^2)^{-1}, \tag{4.4}$$

with the amplitude f_n describing the integral intensity and $2\Gamma_n$ the linewidth of the corresponding Lorentzian contribution to the spectrum. The index zero is chosen to denote the resonant line, i.e., the line with (half) linewidth $\Gamma_0 = \Gamma/2$. We will compare the temperature dependence of the amplitude f_0 of the resonant line, i.e., the *Lamb–Mössbauer factor*, and the amplitude f_1 and linewidth Γ_1 of the first broadened line with the experimental data of Parak *et al.*[44,45]; the third line in the approximated spectrum can be viewed as the background.

The generalized moments $\mu_0, \mu_{-1},\ldots,\mu_{-5}$ employed in the approximation were calculated using the method of Sec. III. In case of a three-dimensional motion equations (3.4b) have a cylindrical symmetry around the axis defined by vector $\mathbf{k}$ and, therefore, the problem of the determination of the auxiliary functions can be reduced to a two-dimensional one. A substitution of the radially symmetric equilibrium distribution $p_0(r) = p_0(\rho, z)$ by

$$p_0'(\rho, z) = \rho p_0(\rho, z), \quad \rho = (x^2 + y^2)^{1/2}, \tag{4.5a}$$

brings the adjoint operator into the form

$$\begin{aligned} L^+(\rho, z) &= D\{[\rho p_0(\rho, z)]^{-1}\partial_\rho [\rho p_0(\rho, z)]\partial_\rho \\ &\quad + p_0(\rho, z)^{-1}\partial_z\, p_0(\rho, z)\partial_z\} \\ &= D\{p_0'(\rho, z)^{-1}\partial_\rho\, p_0'(\rho, z)\partial_\rho \\ &\quad + p_0'(\rho, z)^{-1}\partial_z\, p_0'(\rho, z)\}. \end{aligned} \tag{4.5b}$$

In this form a discretization of the operator according to Sec. III is possible. In the numerical calculations the infinite diffusion space was limited to a rectangle $[0, \rho_{\max}] \times [-z_{\max}, z_{\max}]$, corresponding to a section through a cylinder of height $2z_{\max}$ and radius $\rho_{\max}$. This rectangle was divided into 71×141 cells. The choice of an odd number of cells is necessary to take into account properly the contribution from the, possibly small, central substate. The value of $z_{\max}$ was chosen to be

$$z_{\max} = 3\langle r^2\rangle^{1/2} \tag{4.6}$$

with $\langle r^2\rangle$ the mean half-width of the stationary distribution

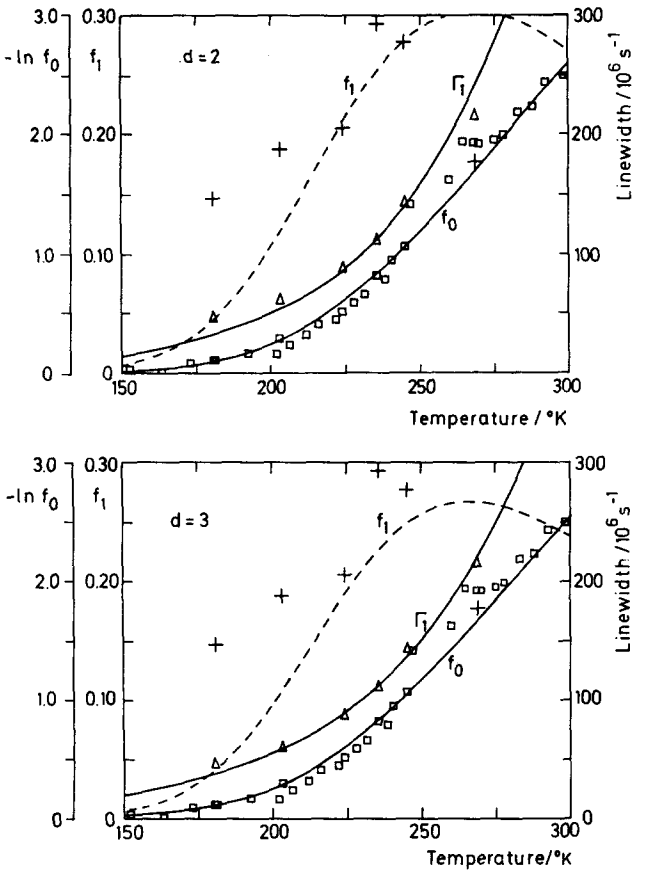

FIG. 3. Comparison of the observed (Refs. 44 and 45) temperature dependence of the Mössbauer spectrum from myoglobin with the spectrum predicted from our stochastic model (see the text) in $d = 2$ and $d = 3$ (parameters see Table I); f_0 denotes the Lamb–Mössbauer factor (□,–), i.e., the amplitude of the resonant line; f_1 denotes the amplitude (+ ,---) and Γ_1 the width (△,–) of the broadened line. As done in Refs. 45 and 18, the amplitude for a superimposed harmonic mode has been subtracted from the data for f_0.

in the harmonic envelope potential. This choice is a good compromise for potentials whose large-distance behavior is given by a harmonic potential. The value of $\rho_{\max}$ is determined from the discretization length δ resulting from Eq. (4.6) and the number of discretization points; it has almost the same value as $z_{\max}$.

In case of a two-dimensional motion we limited the diffusion space to the square $[-x_{\max}, x_{\max}] \times [-y_{\max}, y_{\max}]$, divided into 101×101 cells, with $x_{\max}$ and $y_{\max}$ determined by Eq. (4.6). We may note that the above discretizations result in matrix operators with a dimension N of order 10^4, a size that would not be tractable by other than sparse matrix techniques.

Figure 3 shows a comparison of the temperature dependence of the spectrum obtained from our model with the experimental results. The corresponding parameters which provided the best agreement with the observations are given in Table I and compared with the parameters from the one-dimensional model of Ref. 18. The theoretical predictions agree well with the observations. Discrepancies are found only for the amplitude f_1 of the broadened line. These can in part be attributed to a certain arbitrariness in the determination of the contribution of the background in the theoretical description as well as in the observations. However, the qualitative temperature dependence and the magnitude of the contribution of this line is reproduced correctly.

A comparison of the parameters for models (4.1) and (4.2) in different dimensions shows them to be rather independent of the dimension of the diffusion space, with the exception of the quantity s_0. The values for the energy of the substate and the prefactor as well as the activation energy of the diffusion coefficient (4.1) are comparable to those already obtained in case of the one-dimensional model. The values for the linear extension s_0 of the substate depend strongly on the dimension. For $d = 1$ the rather unphysical small value of 2.0×10^{-4} Å had been obtained in Ref. 18. For the two- and three-dimensional descriptions provided here this parameter is about 10^{-2} Å, a value more appropriate in comparison with interatomic distances. We may note, though, that the value for s_0 for the three-dimensional description probably is too high since in the discretized form of the cylindrical symmetric problem (3.4b) the contribution from the energetically lowest part of the substate is taken into account insufficiently. For an interpretation of the extensions of the stable substate one should compare the volume of this substate with the average volume accessible to thermal motion. The ratio of these volumes is approximately given by

$$\Omega_{\text{rel}} \approx (s_0^2/\langle r^2 \rangle)^{d/2}, \tag{4.7}$$

with $\langle r^2 \rangle$ the mean half-width of the thermal distribution in the harmonic envelope potential. This ratio is rather independent of the dimension and assumes at room temperature the values $\Omega_{\text{rel}} \approx 0.6 \times 10^{-3}$, 10^{-3}, and 5×10^{-3} for $d = 1,2$, and 3, respectively.

For a more detailed discussion of the results above con-

TABLE I. Parameters for the description of observed Mössbauer spectra from myoglobin using our stochastic model (see the text) with diffusion coefficient (4.1) and potential (4.2).

	Central substate		Effective diffusion coefficient	
Dimension	Energy difference $\Delta E/k_B$[K]	Linear extension s_0[Å]	Diffusion coefficient D_0[10^8Å^2/s]	Activation energy E_0/k_B[K]
$d = 1$[a]	1900	2.0×10^{-4}	8.3	1100
$d = 2$	1875	1.0×10^{-2}	11.0	1000
$d = 3$	1950	5.6×10^{-2}	11.0	1000

[a]Data from Ref. 18; s_0 corresponds to the quantity $(\pi/2)^{1/2} \exp(-\Delta S/k_B) l_{ss}$ in that reference.

cerning the implications for protein dynamics and a comparison with molecular dynamics studies we refer to Ref. 18 and a forthcoming publication.[46]

ACKNOWLEDGMENT

This project has been supported by the Deutsche Forschungs Gemeinschaft (Schu 523).

APPENDIX A: COMPARISON OF THE COMMON DISCRETIZATION SCHEME FOR THE FOKKER–PLANCK OPERATOR WITH THE DISCRETIZATION VIA AN EQUIVALENT MASTER EQUATION OPERATOR

To clarify the essential points it is sufficient to limit the considerations to the one-dimensional case. For simplicity, we neglect a discussion of boundary conditions and assume a position-independent diffusion coefficient D. In this case, the FPO (2.1c) can be written in the form

$$L(x) = D\,[(\partial^2/\partial x^2) + \beta\, U'(x)(\partial/\partial x) + \beta\, U''(x)]. \quad \text{(A1)}$$

In common discretization schemes[26,28] this elliptic operator is approximated by a difference operator $\mathsf{L}^{(c)}$ with the elements

$$L_{ij}^{(c)} = \begin{cases} D\,[2\delta^{-2} + \beta U''(x_i)] & \text{for } j = i, \\ D\,[\delta^{-2} \pm \delta^{-1}\beta U'(x_i)/2] & \text{for } j = i \pm 1, \\ 0 & \text{otherwise,} \end{cases} \quad \text{(A2)}$$

where δ is the discretization length and $x_i = x_{\min} + (2i-1)\delta/2$ in case the discretization points are chosen according to Sec. III. As can be shown easily using Taylor expansion, the matrix operator $\mathsf{L}^{(c)}$ is a *second-order approximation* to $L(x)$ in the sense that the following relation holds:

$$L(x_i)f(x_i) = (\mathsf{L}^{(c)}\mathbf{f})_i + O(\delta^2). \quad \text{(A3)}$$

This common form of discretization has some important disadvantages. In particular, the matrix operator $\mathsf{L}^{(c)}$ has lost some essential properties of the FPO (A1). First of all, the conservation of total probability is not guaranteed anymore:

$$\frac{d}{dt}p_{\text{ges}}(t) = \frac{d}{dt}\mathbf{1}^T\mathbf{p}(t)$$
$$= \mathbf{1}^T\mathsf{L}^{(c)}\mathbf{p}(t) = O(\delta^2) \neq 0 \quad \text{in general.} \quad \text{(A4)}$$

This follows from the fact that the sums over the columns of the matrix operator do not vanish in general, i.e.,

$$(\mathbf{1}^t\mathsf{L}^{(c)})_j = \sum_i L_{ij}^{(c)} = O(\delta^2) \quad \text{for all } j, \quad \text{(A5)}$$

as can be shown by Taylor expansion. This limitation becomes relevant for potentials with anharmonicities of at least fourth order, since the leading term on the right-hand side of Eq. (A5) is given by $U^{(4)}(x)$. Properties (A4) and (A5) are equivalent to the fact that the discretized stationary probability distribution $\mathbf{p}_0$ is, in general, *not* the eigenvector of $\mathsf{L}^{(c)}$ with the eigenvalue zero, i.e.,

$$(\mathsf{L}^{(c)}\mathbf{p}_0)_i = (\mathbf{p}_0)_i O(\delta^2) \quad \text{for all } i. \quad \text{(A6)}$$

Correspondingly, the condition of *detailed balance* does not hold, i.e.,

$$L_{ij}^{(c)}(\mathbf{p}_0)_j \neq L_{ji}^{(c)}(\mathbf{p}_0)_i \quad \text{in general.} \quad \text{(A7)}$$

Therefore, in the numerical evaluation of quantities that are determined by the stationary distribution (or by the zero eigenvalue) errors can occur. Besides, in case of numerical long-time integration of the FPE with the help of $\mathsf{L}^{(c)}$ instabilities may appear, e.g., the probability distributions may diverge or vanish. These problems can be avoided only if very small values of δ are chosen.

In addition, the matrix operator $\mathsf{L}^{(c)}$ cannot be symmetrized, whereas this is possible for the original FPO (A1) in the sense that Eq. (A1) can be transformed into a self-adjoint operator.[3] This problem could be circumvented by discretizing the symmetric form of $L(x)$

$$L^{(s)}(x) = [p_0(x)]^{-1/2} L(x) [p_0(x)]^{1/2}$$
$$= D\,\{\partial^2/\partial x^2) - [\tfrac{1}{2}\beta U'(x)]^2 + \tfrac{1}{2}\beta U''(x)\}. \quad \text{(A8)}$$

However, the limitations (A4) to (A7), discussed above, hold in an equivalent form for such a symmetric matrix operator.

Furthermore, in some cases the condition of *nonnegativity*,

$$L_{ij}^{(c)}/L_{ii}^{(c)} \leqslant 0, \quad i \neq j, \quad \text{(A9)}$$

a property that guarantees convergence of some numerical methods,[26] is fulfilled only for very small values of δ.

All these properties, arising from the discretization (A2), lead to numerical problems which superpose the inherent problems deriving from the numerical methods employed and from the finite precision of the numerical computation.

As can be shown easily, the master equation operator $\mathsf{L}^{(M)}$ does not have these disadvantages. For the FPO (A1) $\mathsf{L}^{(M)}$ assumes the form

$$L_{ij}^{(M)} = \begin{cases} -(L_{i-1,i}^{(M)} + L_{i+1,i}^{(M)}) & \text{for } j = i, \\ \tau^{-1}[(\mathbf{p}_0)_i/(\mathbf{p}_0)_{i\pm1}]^{1/2} & \text{for } j = i \pm 1, \\ 0 & \text{otherwise.} \end{cases} \quad \text{(A10)}$$

In particular, the following properties hold:

(i) $\mathsf{L}^{(M)}$ is a second-order approximation to Eq. (A1), in the sense of Eq. (A3) and, therefore, has the same convergence properties as $\mathsf{L}^{(c)}$:

(ii) $\mathsf{L}^{(M)}$ conserves the total probability since, because of Eq. (A10), the following relation holds:

$$\mathbf{1}^T\mathsf{L}^{(M)} = \mathbf{0}; \quad \text{(A11)}$$

in particular, $\mathbf{p}_0$ is the eigenvector of $\mathsf{L}^{(M)}$ with eigenvalue zero and detailed balance holds.

(iii) $\mathsf{L}^{(M)}$ can be symmetrized acording to Eq. (3.15).

(iv) $\mathsf{L}^{(M)}$ fulfills the condition of nonnegativity (A9).

In using $\mathsf{L}^{(M)}$, the choice of the discretization length δ is mainly determined by the quality of the approximation and not by the additional criterium of numerical stability. In practical application one notices that, in comparison to the use of $\mathsf{L}^{(c)}$, one can choose larger values of δ and, therefore, a smaller number of discretization points is sufficient.

We may note that both the conventional discretized operator $\mathsf{L}^{(c)}$ as well as the master equation operator $\mathsf{L}^{(M)}$ do not always have the property of *diagonal dominance*,

$$\sum_{j\neq i} |L_{ij}| \leqslant |L_{ii}| \quad \text{(A12)}$$

which is, besides Eq. (A9), another criterion for conver-

gence of numerical methods.[26,29] However, the discretized adjoint operator $\mathsf{L}^{+(M)}$ is given by the transposed matrix $\mathsf{L}^{(M)T}$. Because of the form (A10), this adjoint operator fulfills condition (A12) with the equality sign. This indicates that it can be numerically safer to calculate the discretized auxiliary functions $\boldsymbol{\mu}_n$ with the use of the adjoint operator rather than with the use of $\mathsf{L}^{(M)}$, which also would be possible (see Ref. 19).

APPENDIX B: DISCRETIZATION OF THE FOKKER–PLANCK OPERATOR IN CASE OF A POSITION-DEPENDENT DIFFUSION COEFFICIENT

In this case the discretization of the operators L and L^+ is very similar to that presented in Sec. III. We use the transformed operators

$$L'(\mathbf{x}) = L(x)\langle D(\mathbf{x})\rangle D(\mathbf{x})^{-1} = \langle D(\mathbf{x})\rangle \nabla \cdot [D(\mathbf{x})p_0(\mathbf{x})]\nabla [D(\mathbf{x})p_0(\mathbf{x})]^{-1}, \tag{B1a}$$

$$L^{+\prime}(\mathbf{x}) = \langle D(\mathbf{x})\rangle D(\mathbf{x})^{-1}L^+(x) = \langle D(\mathbf{x})\rangle [D(\mathbf{x})p_0(\mathbf{x})]^{-1}\nabla \cdot [D(\mathbf{x})p_0(\mathbf{x})]\nabla. \tag{B1b}$$

This transformation is possible since $D(\mathbf{x})$ does not vanish. The transformed operators L' and $L^{+\prime}$ have a structure comparable to that of Eqs. (2.5) and (2.11), respectively, with a constant diffusion coefficient which is a prerequisite for the discretization according to Sec. III. The constant diffusion coefficient is given by the global thermal average of $D(\mathbf{x})$,

$$D' = \langle D(\mathbf{x})\rangle, \tag{B2}$$

and the stationary distribution $p_0(\mathbf{x})$ is replaced by the transformed distribution

$$p_0'(\mathbf{x}) = D(\mathbf{x})p_0(\mathbf{x}). \tag{B3}$$

The operators L' and $L^{+\prime}$ can, therefore, readily be discretized to master equation operators $\mathsf{L}^{(M)'}$ and $\mathsf{L}^{+(M)'}$, respectively, using the method of Sec. III. In particular, $\mathsf{L}^{(M)'}$ and $\mathsf{L}^{+(M)'}$ have all the convenient properties discussed there.

However, because of the transformations (B1) the discretized Fokker–Planck equation (3.10) and Eqs. (3.17) and (3.18) for the determination of the discretized auxiliary functions $\boldsymbol{\mu}_n$ now assume slightly different forms.

For Eq. (3.10) we get

$$\partial_t \mathbf{p} = \mathsf{L}^{(M)'}\mathsf{D}\,\mathbf{p}, \tag{B4}$$

where D is a diagonal matrix with

$$D_{i,j} = \delta_{i,j}D(\mathbf{x}_i)/D'. \tag{B5}$$

Equation (B4) can be used for the numerical integration of the FPE since the operator

$$\mathsf{L}^{(M,D)} = \mathsf{L}^{(M)'}\mathsf{D} \tag{B6}$$

is a second-order approximation in the sense of Eq. (A3) to the FPO $L(\mathbf{x})$, as can easily be seen by Taylor expansion. In addition, we may note that $\mathsf{L}^{(M,D)}$ fulfills the condition of detailed balance with respect to $\mathbf{p}_0$, i.e.,

$$L_{i,j}^{(M,D)}(\mathbf{p}_0)_j = L_{i,j}^{(M,D)}(\mathbf{p}_0)_i \quad \text{for all } \mathbf{i}, \mathbf{j}, \tag{B7}$$

which is easily proven using definition (3.8) of the transition rates and employing the transformed distribution (B3).

In an analogous way we get for the discretized auxiliary functions $\boldsymbol{\mu}_n$ the following equations: Eqs. (3.17) for the high-frequency moments change to

$$\boldsymbol{\mu}_n = -\mathsf{D}\mathsf{L}^{+(M)'}\boldsymbol{\mu}_{n-1} \tag{B8a}$$

and

$$\boldsymbol{\mu}_n = -[\mathsf{D}\mathsf{L}^{+(M)'} - \mathsf{K}]\boldsymbol{\mu}_{n-1}, \tag{B8b}$$

respectively, whereas Eqs. (3.18) for the low-frequency moments become

$$\mathsf{D}\mathsf{L}^{+(M)'}\boldsymbol{\mu}_n = -\boldsymbol{\mu}_{-(n-1)} \tag{B9a}$$

and

$$[\mathsf{D}\mathsf{L}^{+(M)'} - \mathsf{K}]\boldsymbol{\mu}_{-n} = -\boldsymbol{\mu}_{-(n-1)}, \tag{B9b}$$

respectively. The application of the numerical algorithms for the solution of these equations discussed in Sec. III is straightforward.

[1] N. G. van Kampen, *Stochastic Processes in Physics and Chemistry* (North-Holland, Amsterdam, 1981).
[2] C. W. Gardiner, *Handbook of Stochastic Methods* (Springer, Berlin, 1983).
[3] H. Risken, *The Fokker–Planck Equation* (Springer, Berlin, 1984).
[4] I. Oppenheim, K. E. Shuler, and G. H. Weiss, *Stochastic Processes in Chemical Physics* (MIT, Cambridge, 1977).
[5] D. Forster, *Hydrodynamic Fluctuations, Broken Symmetry and Correlation Functions* (Benjamin, Reading, Mass., 1975).
[6] *Stochastic Processes–Formalism and Applications*, edited by G. S. Agarwal and S. Dattagupta (Springer, Berlin, 1983).
[7] P. C. Hohenberg and B. I. Halperin, Rev. Mod. Phys. **49**, 435 (1977).
[8] F. W. Wiegel, Phys. Rep. **95**, 283 (1983).
[9] E. Frehland, *Stochastic Transport Processes in Discrete Biological Systems* (Springer, Berlin, 1982).
[10] J. A. McCammon, Rep. Prog. Phys. **47**, 1 (1984).
[11] E. Helfand, Science **226**, 647 (1984).
[12] K. Schulten, A. Brünger, W. Nadler, and Z. Schulten, in *Synergetic—From Microscopic to Macroscopic Order*, edited by E. Frehland (Springer, Berlin, 1984), pp. 80–89. There is a typographical error in Eq. (20) where **a** should be replaced by $\mathbf{a}^N$.
[13] A. Szabo, K. Schulten, and Z. Schulten, J. Chem. Phys. **72**, 4350 (1980).
[14] K. Schulten, Z. Schulten, and A. Szabo, J. Chem. Phys. **74**, 4426 (1981).
[15] B. Carmeli and A. Nitzan, J. Chem. Phys. **76**, 5321 (1982).
[16] A. Brünger, R. Peters, and K. Schulten, J. Chem. Phys. **82**, 2147 (1985).
[17] W. Nadler and K. Schulten, Phys. Rev. Lett. **51**, 1712 (1983).
[18] W. Nadler and K. Schulten, Proc. Natl. Acad. Sci. U.S.A. **81**, 5719 (1984).
[19] W. Nadler and K. Schulten, J. Chem. Phys. **82**, 151 (1985).
[20] W. Nadler and K. Schulten, Z. Phys. B **59**, 53 (1985).
[21] *Sparse Matrix Techniques*, edited by V. A. Barker (Springer, Berlin, 1976).
[22] O. Oesterby and Z. Zlatev, *Direct Methods for Sparse Matrices* (Springer, Berlin, 1983).
[23] G. A. Baker and P. Graves-Morris, *Padé-approximants I, II* (Addison–Wesley, Reading, Mass., 1981).
[24] J. M. Deutch, J. Chem. Phys. **73**, 4700 (1980).
[25] P. J. Davies and P. Rabinowitz, *Methods of Numerical Integration* (Academic, New York, 1975).
[26] G. E. Forsythe and W. R. Wasow, *Finite difference Methods for Partial Differential Equations* (Wiley, New York, 1960).
[27] R. D. Richtmyer and K. W. Morton, *Difference Methods for Initial Value Problems* (Wiley, New York, 1967).
[28] W. F. Ames, *Numerical Methods for Partial Differential Equations* (Barnes & Noble, New York, 1969).
[29] G. Dahlquist, A. Björck, and N. Anderson, *Numerical Methods* (Prentice Hall, Englewood Cliffs, 1974).
[30] S. C. Eisenstat, M. C. Gursky, M. H. Schultz, and A. H. Sherman, *Yale sparse matrix package. I. The Symmetric Codes, II. The Nonsymmetric Codes* (Department of Computer Science, Yale University, 1977), Technical Reports 112 and 114.
[31] S. C. Eisenstat, M. C. Gursky, M. H. Schultz, and A. H. Sherman, Int. J. Num. Meth. Eng. **18**, 1145 (1982).
[32] D. R. Kincaid, J. R. Respess, D. M. Young, and R. G. Grimes, ACM

Trans. Math. Software **8**, 302 (1982).
[33]H. C. Elman, *Iterative Methods for Large Sparse Nonsymmetric Systems of Linear Equations* (Department of Computer Science, Yale University, 1982), Technical report 229.
[34]S. C. Eisenstat, H. C. Elman, and M. H. Schultz, SIAM J. Num. Anal. **20**, 345 (1983).
[35]A. Cooper, Proc. Natl. Acad. Sci. U.S.A. **73**, 2740 (1976).
[36]H. Frauenfelder, G. A. Petsko, and D. Tsernoglu, Nature **280**, 558 (1979).
[37]P. J. Artymiuk, C. C. F. Blake, D. E. P. Grace, S. J. Oately, D. C. Phillips, and M. J. E. Sternberg, Nature **280**, 563 (1979).
[38]C. Careri, P. Fasella, and E. Gratton, Annu. Rev. Biophys. Bioeng. **8**, 69 (1979).
[39]G. R. Welch, B. Somogyi, and S. Damjanovich, Prog. Biophys. Mol. Biol. **391**, 109 (1982).
[40]M. Karplus, Adv. Biophys. **18**, 165 (1984).
[41]S. Adelman, Adv. Chem. Phys. **53**, 61 (1983).
[42]R. H. Austin, L. Beeson, L. Eisenstein, H. Frauenfelder, and I. C. Gunsalus, Biochemistry **14**, 5355 (1975).
[43]K. S. Singwi and A. Sjölander, Phys. Rev. **120**, 1093 (1960).
[44]F. Parak, E. W. Knapp, and D. J. Kucheida, J. Mol. Biol. **161**, 177 (1982).
[45]E. W. Knapp, S. F. Fischer, and F. Parak, J. Phys. Chem. **86**, 5042 (1982).
[46]W. Nadler, A. Brünger, K. Schulten, C. L. Brooks, and M. Karplus (to be submitted).